Available online at www.sciencedirect.com
ScienceDirect
Bioorganic & Medicinal Chemistry Letters 18 (2008) 3224–3229
Bioorganic & Medicinal Chemistry Letters

Discovery of orally active pyrrolopyridine- and aminopyridine-based Met kinase inhibitors

Zhen-Wei Cai,* Donna Wei, Gretchen M. Schroeder, Lyndon A. M. Cornelius, Kyoung Kim, Xiao-Tao Chen, Robert J. Schmidt, David K. Williams, John S. Tokarski, Yongmi An, John S. Sack, Veeraswamy Manne, Amrita Kamath, Yueping Zhang, Punit Marathe, John T. Hunt, Louis J. Lombardo, Joseph Fargnoli and Robert M. Borzilleri

Bristol-Myers Squibb Research and Development, PO Box 4000, Princeton, NJ 08543-4000, USA

Received 29 February 2008; revised 21 April 2008; accepted 22 April 2008
Available online 25 April 2008

Abstract—A series of acylurea analogs derived from pyrrolopyridine and aminopyridine scaffolds were identified as potent inhibitors of Met kinase activity. The SAR at various positions of the two kinase scaffolds was investigated. These studies led to the discovery of compounds **3b** and **20b**, which demonstrated favorable pharmacokinetic properties in mice and significant antitumor activity in a human gastric carcinoma xenograft model.

Met is a receptor tyrosine kinase protein that has a high binding affinity for hepatocyte growth factor/scatter factor (HGF/SF).[1] Upon activation with its endogenous ligand HGF/SF, Met mediates various cellular responses, such as epithelial cell dissociation (scattering), invasion, tubular morphogenesis, and angiogenesis.[2] While Met/HGF signaling is essential for normal physiological events, such as placental development and liver regeneration,[3] aberrant activation of this pathway is reported to lead to tumorigenicity and metastasis.[4,5] Due to the prevalence of Met amplification/overexpression and mutations in a variety of human malignancies, inhibition of Met kinase activity by small molecules or biologics would likely have broad therapeutic utility.[6] Several reports have already indicated that inhibition of Met kinase activity blocks tumor cell growth and invasion in both in vitro and in vivo systems.[7]

Recently, we disclosed a series of potent Met kinase inhibitors with malonamide **1a** and acylurea **1b** groups substituted on the pyrrolo[2,1-*f*][1,2,4]triazine scaffold (Fig. 1).[8] However, due to poor pharmacokinetic properties associated with compounds **1**, we investigated additional kinase inhibitor templates such as the pyrrolopyridine **2** and aminopyridine **3** (Fig. 1). These chemotypes also mimic the adenine group of ATP and allow for the design of potent Met kinase inhibitors. In this report, we describe the SAR optimization and in vivo assessment of selected pyrrolopyridine- and aminopyridine-based Met kinase inhibitors.

As shown in Table 1, two assays were used to evaluate the activity of initial pyrrolopyridine and aminopyridine analogs, **2** and **3**, respectively. The Met kinase assay measured the ability of a compound to inhibit enzymatic activity of the Met receptor. The GTL-16 cellular assay was used to assess the ability of the compounds to inhibit the proliferation of this Met-driven (amplified Met) human gastric carcinoma cell line. Both the malonamide-substituted pyrrolopyridine analog **2a** and the aminopyridine analog **3a** demonstrated superior biochemical potency compared to the pyrrolotriazine analog **1a**. The malonamide derivatives **2a** and **3a** possessed potency comparable to the corresponding acylurea analogs (**2b** and **3b**) in the enzymatic assay; however, they exhibited only moderate antiproliferative activity in the cellular assay. The acylurea-substituted pyrrolopyridine analog **2b** displayed potent inhibition of Met kinase activity with an IC_{50} value of 110 nM, whereas the corresponding aminopyridine analog **3b** was three-fold more potent than **2b**. In the GTL-16 cellular proliferation assay, **2b** provided nearly a two-fold

Keywords: Met; Receptor tyrosine kinase; Protein kinase inhibitors.
* Corresponding author. E-mail: zhenwei.cai@bms.com

0960-894X/$ - see front matter © 2008 Elsevier Ltd. All rights reserved.
doi:10.1016/j.bmcl.2008.04.047

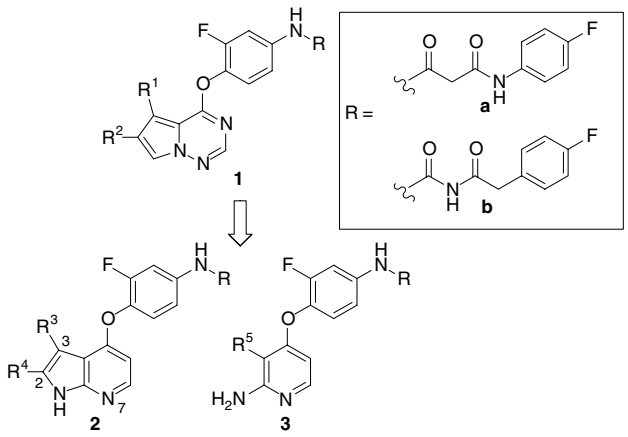

Figure 1. Met kinase inhibitors derived from different scaffolds.

Table 1. In vitro activities of compounds **1b**, **2**, and **3**[a]

Compound	IC_{50} (μM)	
	Kinase	GTL-16
1a (R^1 = Me, R^2 = H)	0.78	—
2a (R^3 = R^4 = H)	0.064	1.06
2b (R^3 = R^4 = H)	0.11	0.15
3a (R^5 = H)	0.10	1.49
3b (R^5 = H)	0.035	0.29

[a] For assay conditions, see Ref. 8.

increase in potency relative to **3b**. Consistent with the SAR observed in the series of pyrrolotriazine derivatives **1**,[8] the analogs with an acylurea moiety (**2b** and **3b**) in both the aminopyridine and pyrrolopyridine series provided 5- to 10-fold better cellular potency than those corresponding analogs with malonamide substitution (**2a** and **3a**). Therefore, the SAR of only the acylurea-substituted pyrrolopyridines and aminopyridines was investigated further.

The synthesis of compound **2a** was accomplished by standard amide bond coupling of aniline intermediate **4**[9] and acid intermediate **5** as shown in Scheme 1. Treatment of **4** with acylisocyanate **6**[8] gave rise to **2b** in moderate yield. Aminopyridine analogs **3a** and **3b** were obtained in a similar manner as **2a** and **2b** using the corresponding aniline **7**.[10]

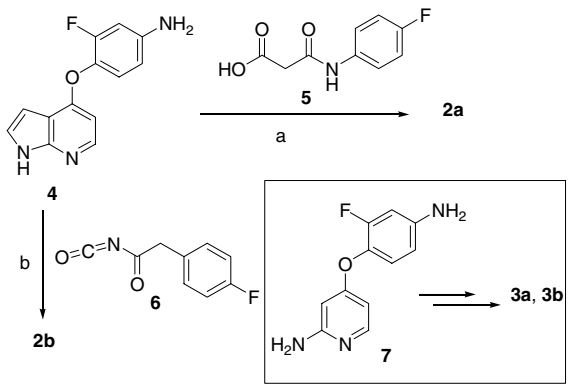

Scheme 1. Reagents and conditions: (a) PyBOP, DIPEA, THF, rt, 75–90%; (b) DCM, rt, 65–75%.

Introduction of substituents at the C3 position of pyrrolopyridine intermediate **8**[9] was accomplished using chemistry illustrated in Scheme 2. A Friedel-Crafts reaction of **8** with bromoacetyl chloride in the presence of $AlCl_3$ afforded bromoacetyl ketone **9**, which was treated with the corresponding amines to provide the intermediates **10**. Subsequent reduction of nitro group with zinc powder and NH_4Cl in MeOH, followed by treatment with acylisocyanate **6**, provided compounds **11a**, **b**, **c**. The synthesis of trichloromethyl ketone intermediate **12** was also carried out by a Friedel-Crafts reaction. Compound **13** was prepared from **12** using a similar reaction sequence for **11**. Treatment of **13** with 3-aminomethylpyridine in DMF gave the amide analog **14**. Reaction of **12** with NaOH in MeOH afforded the ester intermediate **15**. The ester analog **16** was obtained in a similar manner as described for **11**. Reduction of ester **16** with DIBAL in THF yielded the hydroxymethyl analog **17**.

The preparation of compound **20** is outlined in Scheme 3. The pyrrolopyridine intermediate **8** was protected with a SEM group, and brominated with NBS in acetonitrile to give intermediate **18**. Palladium-catalyzed Suzuki coupling of bromo-intermediate **18** with aryl boronic acid afforded the intermediate **19**, which was readily converted to compound **20**[13] in a three-step consecutive sequence involving reduction of nitro group with Zn/NH_4Cl in MeOH, followed by deprotection of the SEM group with TBAF, and subsequent acylurea formation with **6**.

Incorporation of the pyridyl group at the C2 position of pyrrolopyridine **24** was achieved by a Sonogashira reaction[11] of intermediate **21**[10] with 3-ethynylpyridine to give **22**. The intermediate **23** was obtained by reduction of **22** with Zn/NH_4Cl, and pyrrolopyridine formation in the presence of KO^tBu in NMP at elevated temperature.[12] Acylurea formation was carried out in a similar manner as depicted for **20**, to provide desired analog **24**.

The chemistry to introduce substituents at the C3 position of the aminopyridine core is outlined in Scheme 4.[10] A Sonogashira reaction of **21** with various alkynes gave rise to intermediates **25**. The preparation of compounds **26** was carried out using a similar reaction sequence as described for **16**and followed by appropriate functional group transformation as in the preparation of **26e, g**.

The selected pyrrolopyridine analogs depicted in Table 2 were screened and optimized for Met kinase inhibitory activity and anti-proliferation activity versus the GTL-16 cell line. Various C3 and C2 substituents on the pyrrolopyridine core were well tolerated based on the enzymatic activity, and thus provided dramatically increased potency relative to unsubstituted analog **2b**. However, the compounds in Table 2 displayed significant differences in cellular potency. The α-aminoacetyl substitutions as in **11a**, **b**, **c** were 2- to 10- fold more potent than **2b** in the enzyme assay, but they suffered from more than 10-fold loss in inhibitory potency in the GTL-16 proliferation assay, presumably due to poor cell

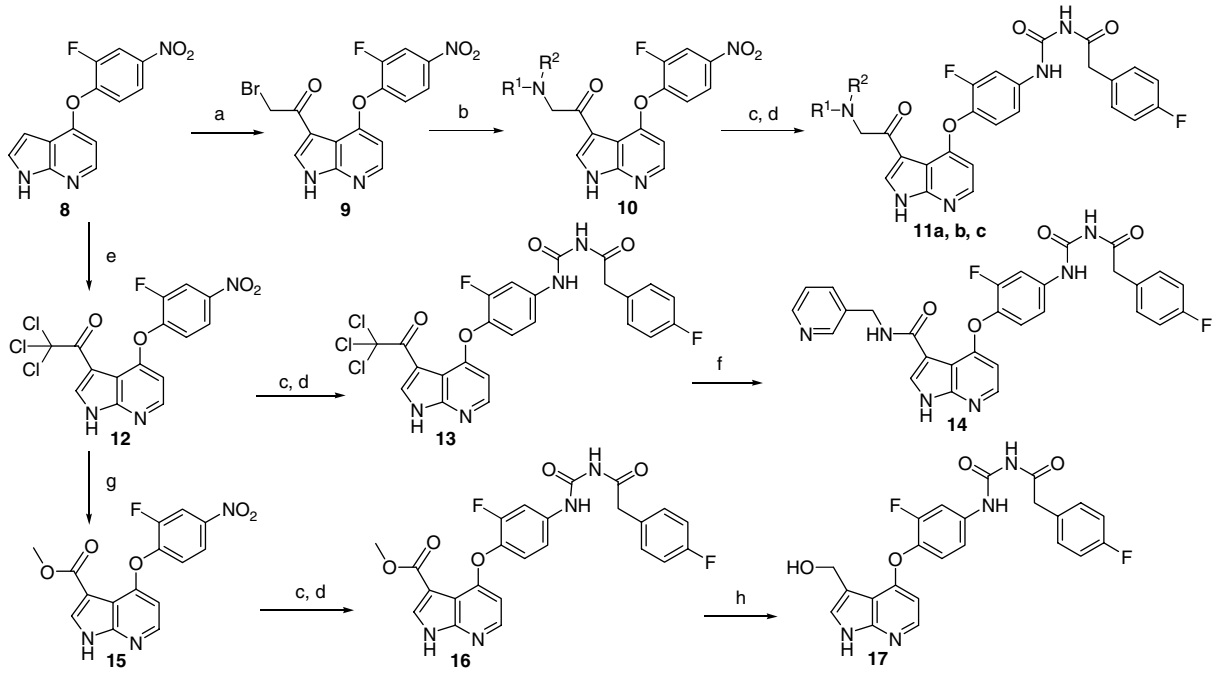

Scheme 2. Reagents and conditions: (a) 2-bromoacetyl chloride, $AlCl_3$, DCE, rt, 78%; (b) R^1R^2NH, THF, rt, 65–90%; (c) Zn, NH_4Cl, MeOH/THF, rt, 70–95%; (d) **6**, DCM, rt, 30–55%; (e) trichloroacetyl chloride, $AlCl_3$, DCE, rt, 76%; (f) 3-aminomethylpyridine, DMF, rt, 61%; (g) 1 N NaOH, MeOH, 61%; (h) DIBAL, THF, 0 °C, 53%.

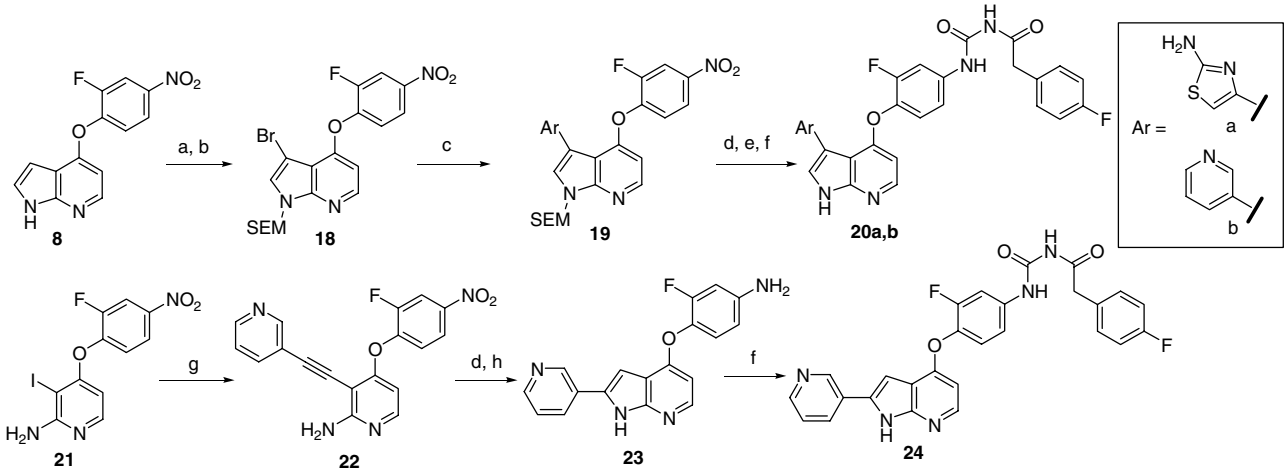

Scheme 3. Reagents and conditions: (a) NaH, SEM-Cl, DMF, −40 to 0 °C; (b) NBS, CH_3CN, 0 °C to rt, 92% for two steps; (c) aryl boronic acid, $Pd(PPh_3)_4$, K_3PO_4, EtOH, toluene, 80 °C, 75–82%; (d) Zn, NH_4Cl, MeOH/THF, rt, 80–95%; (e) TBAF, THF, 50 °C, 78–80%; (f) **6**, DCM, rt, 30–55%; (g) 3-ethynylpyridine, $Pd(PPh_3)_4$, CuI, Et_3N, DMF, 85 °C, 61%; (h) KO^{t}Bu, NMP, 80 °C, 80%.

permeability. The pyridylmethyl amide analog **14** presents with similar potency to **11c** in the enzymatic assay with an IC_{50} value of 11 nM. The weakly basic pyridyl amide analog **14** exhibited enhanced cellular potency as compared to **11a–c**. The methyl ester and hydroxymethyl analogs (**16** and **17**) demonstrated potent Met kinase inhibition with IC_{50} values of 5 and 4 nM, respectively. Compounds **16** and **17** also displayed good cellular potency in the GTL-16 assay. Introduction of heteroaryl groups directly at C3 (analogs **20a** and **20b**) dramatically increased potency, especially in the GTL-16 assay with in vitro IC_{50} values of 30 and 20 nM, respectively. Inspired by the potency gained with the C3 pyridyl-substituted analog **20b**, the C2 pyridyl analog **24** was also evaluated. Compound **24** demonstrated comparable enzymatic and cellular potency to **20b**. Analysis of the X-ray co-crystal structures of compounds **2b** (Fig. 2) and **3b** complexed with the Met kinase domain, reveals that both inhibitors bind in a similar fashion as pyrrolotriazine **1**.[8] These compounds occupy the ATP binding site where the protein is in an inactive conformation. The N7 nitrogen of pyrrolopyridine **2b** accepts a hydrogen bond from the hinge region backbone NH of Met1160, while the pyrrole NH donates a hydrogen bond to the carbonyl of Met1160. The aminophenol ring and acylurea portion of both

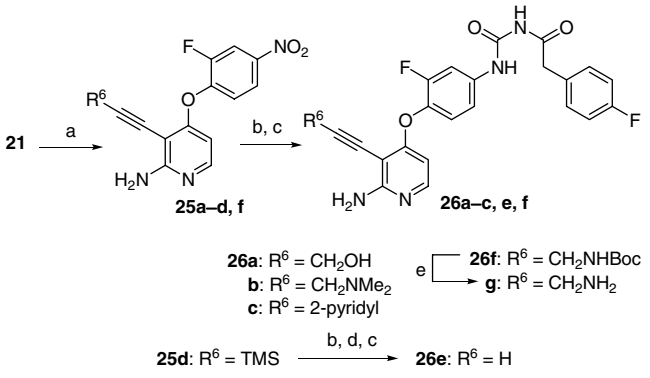

Scheme 4. Reagents and conditions: (a) R^6–CCH, $Pd(PPh_3)_4$, CuI, Et_3N, DMF, 85 °C, 50–80%; (b) Zn, NH_4Cl, MeOH/THF, rt, 70–95%; (c) **6**, DCM, rt, 18–55%; (d) TBAF, THF, −30 to 0 °C, 88%; (e) 35% TFA in DCM, rt, 60%.

inhibitors bind similarly to previously discussed inhibitors.[8] The C3 position of the pyrrolopyridine ring points toward the ribose pocket and the C2 position leads to the surface-exposed extended hinge region. Before interacting with the mixed-polarity solvent-accessible area of the protein, the C2 and C3 substituents must first bypass the steric demand of the mostly hydrophobic pinched-in area of the protein, that is, the bite between the P-loop and extended hinge region comprised of residues such as Ile1084 and Gly1163. Analogs in Table 2 likely satisfy this requirement and thus, have the opportunity to increase interactions with the protein surface. Specifically, the pyridyl analogs **20b** and **24** optimize the interactions with protein in the solvent-accessible pockets and provide dramatic improvement in kinase inhibitory activity. These two compounds were evaluated further in pharmacokinetic studies.

The aminopyridine core of **3b** engages in similar interactions as **2b** with the hinge region (Fig. 2), namely, the backbone NH of Met1160 donates a hydrogen bond to the pyridine N1 and the backbone carbonyl of Met1160 accepts a hydrogen binding from the 2-amino group. The C3 position of the aminopyridine points to the ribose/extended hinge region. The SAR at the C3 position of aminopyridine core was explored by using an alkyne as a spacer to extend groups toward the protein surface. The potential increase in binding affinity was realized, as demonstrated in the improved biochemical activities achieved with aminopyridine analogs **26** (Table 3). The propargyl analog **26a** and the unsubstituted analog **26e** displayed IC_{50} values of low single digit nM in biochemical assay, and IC_{50} values of 30 and 40 nM in the cellular assays, respectively. The basic groups such as Me_2N in **20b** and NH_2 in **20g** provided potent enzymatic activity; however, only moderate cellular activity was observed. Installation of the weakly basic pyridyl group gave the analog **26c** with improved potency in Met kinase and cellular assays. The analogs were subsequently screened for inhibitory activity against an in-house panel of human CYP P450 isozymes. The analogs 26a, **b**, **e**, **g** containing small substituents on the alkyne moiety demonstrated significant inhibition of CYP3A4, whereas **26c** showed only weak activity against CYP3A4 isozyme. Thus, compound **26c** was chosen for further characterization.

Table 2. SAR of pyrrolopyridine series[a]

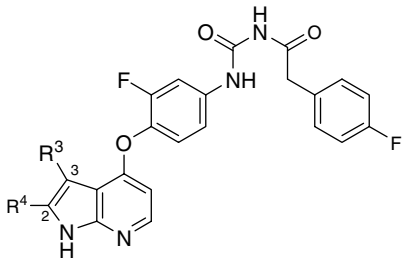

Compound	R^3	R^4	IC_{50} (μM)	
			Kinase	GTL-16
11a	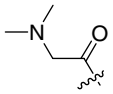	H	0.044	1.05
11b	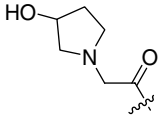	H	0.019	1.47
11c	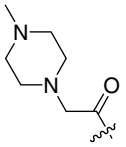	H	0.011	2.22
14	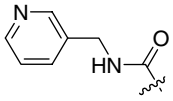	H	0.011	0.65
16		H	0.005	0.18
17		H	0.004	0.18
20a	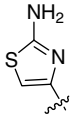	H	0.007	0.03
20b		H	0.002	0.02
24	H	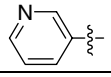	0.002	0.03

[a] For assay conditions, see Ref. 8.

As shown in Table 4, five compounds with potent inhibitory activity in the GTL-16 assay were screened for in vitro metabolic stability using human (HLM) and mouse (MLM) liver microsome systems.[14] Low metabolic rates were observed for all five compounds. Therefore, they were subsequently evaluated in preliminary pharmacokinetic studies in mice (Table 4). Following oral administration of a 50 mg/kg dose, compounds **2b** and **24** demonstrated low plasma levels of drug, whereas **3b**, **20b**, and **26c** yielded moderate to high exposures.

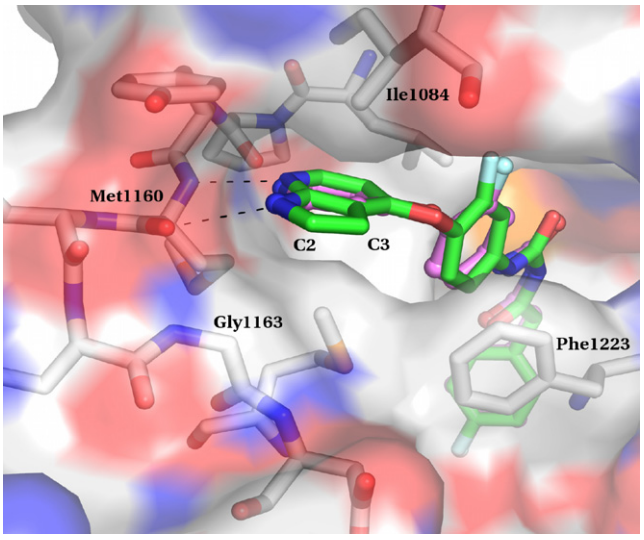

Figure 2. A close-up of the X-ray co-crystal structure of **2b** (in green) and **3b** (in magenta) in the Met ATP binding site (only the protein bound with **2b** is shown). The binding region of the protein is rendered in a surface representation and colored by the associated atoms of the protein (carbon: white, oxygen: red, nitrogen: blue, and sulfur: orange). PDB code: 3CTJ for **2b** and 3CTH for **3b**.

Table 3. SAR of aminopyridine series[a]

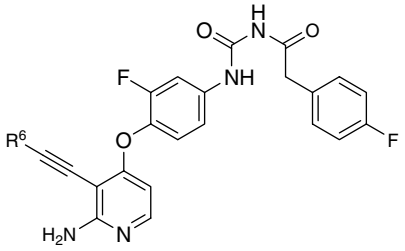

Compound	R^6	IC_{50} (μM)		
		Kinase	GTL-16	CYP3A4
26a	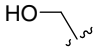	0.003	0.03	0.7
26b	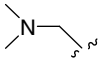	0.004	0.22	2.7
26c	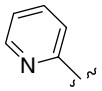	0.005	0.04	37.0
26e	H	0.002	0.04	0.8
26g	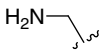	0.005	0.25	1.8

[a] For assay conditions, see Ref. 8.

Based on the high systemic exposures, compounds **3b**, **20b**, and **26c** were further evaluated in an in vivo efficacy study using GTL-16 xenografts implanted in athymic mice.[14] These compounds were administered orally at various dose levels once daily for 14 days, and their percent tumor growth inhibition data (%TGI)[15] are shown in Table 5. Compound **3b** did not demonstrate antitumor activity at a low dose of 25 mg/kg; however, it provided good antitumor activity (%TGI = 80) at the 75 mg/kg dose level and complete tumor stasis (%TGI = 98) at the 125 mg/kg dose level. Compound **26c** exhibited no antitumor activity at the 50 mg/kg dose level, which may be attributed to its high plasma protein binding in mouse (99.98%). Compound **20b** displayed antitumor activity when administered at doses of 50 and 100 mg/kg with %TGI values of 67% and 88%, respectively. Figure 3 represents the dose-dependent tumor growth inhibition of **20b** in GTL-16 model. The 50 mg/kg dose level provided tumor growth delay as compared to the vehicle treated control group, while nearly complete tumor stasis was achieved during the dosing regimen at the 100 mg/kg dose level.

Table 4. Metabolic stability and mouse exposure data following oral administration of selected compounds[a]

Compound	HLM/MLM[a] rate nmol/min/mg	Mouse oral exposure[b,c]			
		C_{max} (μM)[a]	T_{max} (h)	AUC (μM h)	
				(0–4 h)	(0–8 h)
2b	0.015/0.035	2.4	4.0	6.0	—
3b	0.000/0.018	10.5	4.0	33.0	—
20b	0.038/0.049	6.0	4.0	—	34.0
24	0.016/0.036	2.1	4.0	—	11.4
26c	0.000/0.042	16.0	4.0	—	85.0

[a] Compounds at 3 μM incubated in 10 mg of protein (HLM or MLM) for 10 min.
[b] Dosed at 50 mg/kg, all values are means of at least three mice.
[c] Vehicle: PEG400/water (1:1).

Table 5. Antitumor activities of compounds **20b**, **3b**, and **26c** in the GTL-16 xenograft model in mice[a]

Compound	**3b**			**20b**		**26c**
Dose (mg/kg)	25	75	125	50	100	50
%TGI	<50	80	98	67	88	<50

[a] Vehicle: PEG400/water (1:1).

In conclusion, pyrrolopyridine- and aminopyridine-based acylurea analogs proved to be potent inhibitors of Met kinase activity. Compounds **3b** and **20b** demon-

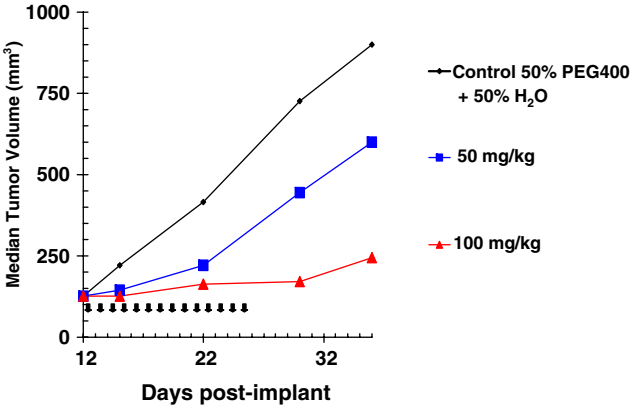

Figure 3. Antitumor activity of **20b** against GTL-16 xenografts implanted in the athymic mice. Arrows indicate dosing.

strated significant anti-tumor activities in human GTL-16 xenograft model in athymic mice.

References and notes

1. Maulik, G.; Shrikhande, A.; Kijima, T.; Ma, P. C.; Morrison, P. T.; Salgia, R. *Cytokine & Growth Factor Rev.* **2002**, *13*, 41.
2. (a) Birchmeier, C.; Gherardi, E. *Trends Cell Biol.* **1998**, *8*, 404; (b) Jiang, W. G.; Martin, T. A.; Parr, C.; Davies, G.; Matsumoto, K.; Nakamura, T. *Crit. Rev. Oncol. Hematol.* **2005**, *53*, 35.
3. (a) Stewart, F. *Rev. Reprod.* **1996**, *1*, 144; (b) Huh, C.-G.; Factor, V. M.; Sanchez, A.; Uchida, K.; Conner, E. A.; Thorgeirsson, S. S. *Proc. Natl. Acad. Sci. U.S.A.* **2004**, *101*, 4477.
4. (a) Jeffers, M.; Rong, S.; Vande Woude, G. F. *Mol. Cell. Biol.* **1996**, *16*, 1115; (b) Matsumoto, K.; Date, K.; Shimura, H.; Nakamura, T. *Jpn. J. Cancer Res.* **1996**, *87*, 702.
5. (a) Edakuni, G.; Sasatomi, E.; Satoh, T.; Tokunaga, O.; Miyazaki, K. *Pathol. Int.* **2001**, *51*, 172; (b) DiRenzo, M. F.; Olivero, M.; Katsaros, D.; Crepaldi, T.; Gaglia, P.; Zola, P.; Sismondi, P.; Comoglio, P. M. *Int. J. Cancer* **1994**, *58*, 658; (c) DiRenzo, M. F.; Olivero, M.; Giacomini, A.; Porte, H.; Chastre, E.; Mirossay, L.; Nordlinger, B.; Bretti, S.; Bottardi, S.; Giordano, S.; Plebani, M.; Gespach, C.; Comoglio, P. M. *Clin. Cancer Res.* **1995**, *1*, 147; (d) For more information regarding the HGF/Met signaling pathway, see http://www.vai.org/met/.
6. (a) Peruzzi, B.; Bottaro, D. P. *Clin. Cancer Res.* **2006**, *12*, 3657; (b) Dussault, I.; Kaplan-Lefko, P.; Jun, T.; Coxon, A.; Burgess, T. L. *Drugs Future* **2006**, *31*, 819; (c) Abidoye, O.; Murukurthy, N.; Salgia, R. *Rev. Recent Clin. Trials* **2007**, *2*, 143; (d) Cui, J. J. *Expert Opin. Ther. Patents* **2007**, *17*, 1035.
7. (a) Wang, X.; Le, P.; Liang, C.; Chan, J.; Kiewlich, D.; Miller, T.; Harris, D.; Sun, L.; Rice, A.; Vasile, S.; Black, R. A.; Howlett, A. R.; Patel, N.; McMahon, G.; Lipson, K. E. *Mol. Cancer Ther.* **2003**, *2*, 1085; (b) Sattler, M.; Pride, Y. B.; Ma, P.; Gramlich, J. L.; Chu, S. C.; Quinnan, L. A.; Shirazian, S.; Liang, C.; Podar, K.; Christensen, J. M.; Salgia, R. *Cancer Res.* **2003**, *63*, 5462; (c) Christensen, J. G.; Schreck, R.; Burrows, J.; Kuruganti, P.; Chan, E.; Le, P.; Chen, J.; Wang, X.; Ruslim, L.; Blake, R.; Lipson, K. E.; Ramphal, J.; Do, S.; Cui, J. J.; Cherrington, J. M.; Mendel, D. B. *Cancer Res.* **2003**, *63*, 7345; (d) Hov, H.; Holt, R. U.; Ro, T. B.; Fagerli, U.-M.; Hjorth-Hansen, H.; Baykov, V.; Christensen, J. G.; Waage, A.; Sundan, A.; Borset, M. *Clin. Cancer Res.* **2004**, *10*, 6686; (e) Zou, H. Y.; Li, Q.; Lee, J. H.; Arango, M. E.; McDonnell, S. R.; Yamazaki, S.; Koudriakova, T. B.; Alton, G.; Cui, J. J.; Kung, P.-P.; Nambu, M. D.; Los, G.; Bender, S. L.; Mroczkowski, B.; Christensen, J. G. *Cancer Res.* **2007**, *67*, 4408.
8. Schroeder, G. M.; Chen, X.-T.; Williams, D. K.; Nirschl, D.; Cai, Z.-W.; Wei, D.; Tokarski, J. S.; An, Y.; Sack, J.; Chen, Z.; Huynh, T.; Vaccaro, W.; Poss, M.; Wautlet, B.; Gullo-Brown, J.; Kellar, K.; Manne, V.; Hunt, J. T.; Wong, T. W.; Lombardo, L. J.; Fargnoli, J.; Borzilleri, R. M. *Bioorg. Med. Chem. Lett.* **2007**, *18*, 1945.
9. Borzilleri, R. M.; Chen, Z.; Huynh, T. N.; Vaccaro, W.; Chen, X.-T.; Kim, K. S. PCT Int. Patent Appl. WO 2006/004636, 2006.
10. Borzilleri, R. M.; Cornelius, L. A. M.; Schmidt, R. J.; Schroeder, G. M.; Kim, K. S. U.S. Patent Appl. 2005/0245530, 2005.
11. Feuerstein, M.; Berthiol, F.; Doucet, H.; Santelli, M. *Synthesis* **2004**, 1281.
12. Rodriguez, A. L.; Koradin, C.; Dohle, W.; Knochel, P. *Angew. Chem. Int. Ed.* **2000**, *39*, 2488.
13. Representative analytical data for **20b**: HPLC R_t = 2.80 min, purity = 98% (Conditions: Phenomenex 5 μm 4.6× 50 mm column, 4 min gradient from 10% to 90% aqueous MeOH with 0.1% TFA, wavelength detected at 220 nM); ^{1}H NMR (500 MHz, DMSO-d_6) δ 12.71 (br s, 1H), 11.04 (br s, 1H), 10.61 (br s, 1H), 9.17 (s, 1H), 8.84 (d, 1H, J = 8.25 Hz), 8.74 (d, 1H, J = 5.50 Hz), 8.20 (d, 1H, J = 5.50 Hz), 8.11 (s, 1H), 8.06 (dd, 1H, J = 8.25, 5.50 Hz), 7.78 (dd, 1H, J = 12.65, 2.20 Hz), 7.50–7.30 (m, 4H), 7.20–7.10 (m, 2H), 6.41 (d, 1H, J = 6.05 Hz), 3.75 (s, 2H); LC–MS (ESI$^+$) m/z 500 (M+H)$^+$; **3b**: HPLC R_t = 1.94 min, purity = 98%; ^{1}H NMR (400 MHz, DMSO-d_6) δ 13.43 (s, 1H), 11.09 (s, 1H), 10.65 (s, 1H), 8.00–7.90 (m, 1H), 7.87–7.83 (m, 2H), 7.48–7.45 (m, 2H), 7.43–7.38 (m, 2H), 7.21–7.15 (m, 2H), 6.71 (dd, 1H, J = 7.23, 2.50 Hz), 6.16 (d, 1H, J = 2.38 Hz), 3.77 (s, 2H); LC–MS (ESI$^+$) m/z 389 (M+H)$^+$; HRMS (M+H)$^+$: found: 399.1258, calcd: 399.1269.
14. For experimental details see: Borzilleri, R. M.; Zheng, X.; Qian, L.; Ellis, C.; Cai, Z.-W.; Wautlet, B. S.; Mortillo, S.; Jeyaseelan, R.; Kukral, D. W.; Fura, A.; Kamath, A.; Vyas, V.; Tokarski, J. S.; Barrish, J. C.; Hunt, J. T.; Lombardo, L. J.; Fargnoli, J.; Bhide, R. S. *J. Med. Chem.* **2005**, *48*, 3991.
15. For a detailed definition for %TGI, see Ref. 14. Antitumor activity of drug is defined as a %TGI > 50%.